Biosensors and Bioelectronics xxx (xxxx) xxx

Contents lists available at ScienceDirect

Biosensors and Bioelectronics

journal homepage: http://www.elsevier.com/locate/bios

Electrochemiluminescence biosensor for DNA hydroxymethylation detection based on enzyme-catalytic covalent bonding reaction of $–CH_2OH$ and thiol functionalized Fe_3O_4 magnetic beads

Chengji Sui, Huanshun Yin **, Lingsong Wang, Yunlei Zhou, Shiyun Ai *

College of Chemistry and Material Science, Shandong Agricultural University, 271018, Taian, Shandong, People's Republic of China

ARTICLE INFO

Keywords:
5-Hydroxymethylcytosine
Electrochemiluminescence biosensor
M. HhaI methyltransferase
Thiol functionalized Fe_3O_4
Chicken embryo fibroblast cell
Rice seedlings

ABSTRACT

5-Hydroxymethylcytosine (5 hmC) is a novel epigenetic modification that plays an important role in mammalian nuclear reprogramming, regulation of gene activity, and initiation of DNA demethylation. In this paper, an electrochemiluminescence sensor was constructed for 5 hmC detection based on thiol functional Fe_3O_4 magnetic beads and covalent chemical reaction of $–CH_2OH$ in 5 hmC. First, Fe_3O_4 magnetic beads were prepared and modified with thiol. Then, 5 hmC was captured on the surface of the magnetic beads by the reaction between $–CH_2OH$ of 5 hmC and –SH of the thiol-functionalized Fe_3O_4 under the catalysis of DNA methyltransferase (M. HhaI). After that, through a series of reactions, phos-tag-biotin, avidin, and bis(hexafluorophosphate) (Ru $(bpy)_2$ (phen-5-NH_2) $(PF_6)_2$) (Ru) were further successively immobilized on the surface of the magnetic beads. More importantly, these reactions were carried out in a solution to ensure the activity of the biomolecules, and further to ensure that the reaction proceeded sufficiently. Finally, an ECL signal was generated by the introduction of Ru. The concentration of 5 hmC presented a good linear relationship with the ECL signal intensity in the range of 0.01–500 nM, and the detection limit was 2.86 pM. Moreover, we also used this method to study the 5 hmC content change in rice seedlings treated with antibiotics and heavy metal composite pollutants, and in chicken embryo fibroblast cell infected with and without avian leukosis virus subgroup J.

1. Introduction

5-Hydroxymethylcytosine (5 hmC) was the hydroxylated form of 5-methylcytosine (5 mC), which can be yield by the oxidization of 5 mC under the catalysis of 10–11 translocation proteins (Song et al., 2010). 5 hmC is the critical intermediate in DNA demethylation, and it is also an important epigenetic modification. It was reported that the level of 5 hmC decreases obviously in some cancers (Chen et al., 2015), which indicated that the 5 hmC may be a biomarker for cancer diagnosis. Moreover, 5 hmC plays a vital role in epigenetic regulation of plants and animals. However, the precise mechanism of 5 hmC is not clear. In order to comprehensively understand the role of 5 hmC in the epigenetic regulation, the method for sensitive and selective detection of 5 hmC is essential.

Various methods have been developed for the detection of 5 hmC, including electrochemistry (Cui et al., 2019), photoelectrochemistry (Sui et al., 2019), electrochemiluminescence (ECL) (Jiang et al., 2018), fluorescence (Hong et al., 2013), single-molecule real-time (SMRT) sequencing (Flusberg et al., 2010), capillary electrophoresis (Krais et al., 2011), high performance liquid chromatography-mass spectrometry (Yin et al., 2015) and thin layer chromatography (Tahiliani et al., 2009). Among these methods, the electrochemiluminescence method has caused widespread concern due to the benefits of easy miniaturization, simple operating, low cost and high sensitivity (Liu et al., 2015). ECL is a chemiluminescence phenomenon induced by electrochemical reaction. Firstly, a certain voltage or current is applied to the system containing chemiluminescent substances. Then, the chemical reaction between the redox products of the electrode or between the electrode redox product and other coexisting substances of the system is carried out to produce the excited state. Finally, the excited state returns to ground state to cause chemiluminescence. Since the energy of the excitation source and the detection signal are completely different, the ECL has a lower background signal and higher sensitivity than electrochemical detection. Due to its combination of electrochemical and optical advantages,

* Corresponding author.
** Corresponding author.
E-mail addresses: yinhs@sdau.edu.cn (H. Yin), ashy@sdau.edu.cn (S. Ai).

https://doi.org/10.1016/j.bios.2019.111908
Received 16 September 2019; Received in revised form 15 November 2019; Accepted 19 November 2019
Available online 23 November 2019

ECL has been widely used in the detection of biomolecule, including chloramphenicol (Miao et al., 2016), microRNA (Feng et al., 2018), adenosine triphosphate (Lu et al., 2013), 5 hmC (Jiang et al., 2018) and cell (Long et al., 2018; Wang et al., 2016). These results demonstrated that the ECL biosensor has prominent application potential for 5 hmC detection.

In ECL sensors, luminescent groups and recognition methods are two important factors. As we all known that Ru $(bpy)_3^{2+}$ and its derivatives are the typical ECL luminescent reagents due to the remarkable stability and strong ECL activity (Sun et al., 2007). For example, Lin et al., has prepared a novel tris(bipyridine)ruthenium (II)-functionalized metal–organic frameworks MOFs to achieve the sensitive detection of Hg^{2+} (Lin et al., 2015). Hu et al., has synthesized Ru-complex-grafted 2D metal-organic layer for detection of mucin 1 (Hu et al., 2019). Cai et al., has used bifunctional ruthenium complex as catalyst and ECL probe to sensitively detect melamine (Cai et al., 2019). Our group also used PAMAM-avidin-Ru as the ECL material to construct the biosensor for 5 hmC detection (Jiang et al., 2018). Owing to the excellent ECL performance of Ru, the ECL biosensor shown good stability and sensitivity.

Due to the similar structure of 5 hmC and 5 mC, it is difficult to distinguish the 5 hmC from 5 mC. Using the covalent reactions of $–CH_2OH$ to detect 5 hmC has become a hot spot, because of the absence of $–CH_2OH$ in 5 mC. More and more enzyme have been used to catalyze the covalent reactions of $–CH_2OH$, such as T4 bacteriophage β-glucosyltransferase (Song et al., 2010) and DNA methyltransferase (M. HhaI) (Liutkevičiūtė et al., 2011). Therefore, using the covalent reactions of $–CH_2OH$ turns out to be a preeminent method to distinguish 5 hmC from 5 mC. However, most biosensors carry out on the electrode surface, which limits the application of biosensor. The steric hindrance effect of the electrode decreases the binding efficiency of biomolecules and biorecognition of target. Moreover, the activity of the biomolecules is affected by temperature, pH and space steric effect on electrode surface (Gao et al., 2017; Ge et al., 2017; Lu et al., 2017), so transferring the reaction on the solution can keep good activity of biomolecules and ensure that the reaction is going to be sufficient.

In recent years, the homogeneous biosensors have attracted widespread attention. The separation was an important part in the homogeneous biosensors. Magnetic separation has become a common separation method due to its advantages of simple operation, low cost and fast separation speed. Recently, Fe_3O_4 has attracted great concentration in analytical area due to their superior properties, such as low toxicity, good biocompatibility, catalytic activity and magnetic separation (Li et al. 2016, 2017). However, Fe_3O_4 can absorb the phosphate group to affect the detection of 5 hmC (Sun et al., 2017; Yan et al., 2015). Thus, Fe_3O_4 was coated with polydopamine (PDA) in this work. The PDA can form a uniform film on the surface of Fe_3O_4, which not only can inhibit the absorption of phosphate group, but also can introduce many specific functional groups by the abundant functional group of PDA. In this work, Fe_3O_4@PDA functionalized with –SH (Fe_3O_4-SH) was synthesized and used as the 5 hmC immobilized substrate and magnetic separation medium to achieve the sensitive detection of 5 hmC. The method shows good stability and sensitivity. In traditional biosensors, biomolecules are modified on the electrodes by layer assembly. However, the capture efficiency is low due to the steric effect of the electrode surface and the influence of biomolecule activity. So, the reactions in this biosensor were carried out in the solution to improve the capture efficiency. Moreover, compared with some previous work, this work is focusing on the detection of single 5 hmC base, not 5 hmC in a DNA sequence, which improve the applicability of this electrochemiluminescence method. As we all known that the traditional electrochemiluminescence method for 5 hmC detection is focusing on the 5 hmC in a DNA sequence. Due to that the single-stranded bases and lengths in animals and plants are unknown, it is difficult to detect 5 hmC in actual animals and plants. However, the 5 hmC content change in chicken embryo fibroblast cell infected with and without avian leukosis virus subgroup J (ALV-J) was detected successfully by this method, indicating the excellent practicality of the biosensor.

2. Experimental section

2.1. Reagents and apparatus

See Supplementary Material.

2.2. Preparation of thiol functional Fe_3O_4 magnetic bead

Fe_3O_4 was prepared by the hydrothermal method (Deng et al., 2005). Firstly, 1.35 g $FeCl_3{\cdot}6H_2O$ was added into 40 mL ethylene glycol and stirred to form a homogeneous solution. Then, 3.6 g sodium acetate and 1.0 g polyethylene glycol were added into the solution. After stirring for 30 min, the solution was transferred into teflon-lines stainless steel autoclave and keep at 200 °C for 8 h. Finally, the product was washed with ethanol for several times, and collected by centrifugation. The solid product was then dried at 60 °C for further use.

The preparation process of Fe_3O_4-SH is as follows. Firstly, 0.5 g Fe_3O_4 was added into 100 mL Tris-HCl (pH = 8.5) solution. Then, 200 mg dopamine hydrochloride was added into the solution and stirred for 2 h. Next, the product was washed with distilled water for several times and collected by centrifugation. Subsequently, the product and 0.1 g 4-mercaptophenylboronic acid were added into 50 mL ethanol/distilled water mixed solution (v/v, 1:1). After stirring for 5 h, the product was washed with distilled water and ethanol for several times. Finally, the product was dried at 60 °C under vacuum and ground into powder before use.

2.3. Preparation of the biosensor

Firstly, Fe_3O_4-SH dispersion was prepared by dispersing 10 mg Fe_3O_4-SH in 5 mL sterilized water with the aid of ultrasonication for 30 min. Then, 40 μL of 2 mg/mL Fe_3O_4-SH dispersion, 20 μL M. HhaI reaction buffer containing 100 unit/mL M. HhaI and 40 μL different concentration 5 hmC were added into sterilized centrifuge tube. The reaction was carried out at 37 °C under shaking. After 140 min, the prepared solid product (it was denoted as Fe_3O_4-5 hmC) was collected by magnetic separation, where the supernate was discarded. Then, the product was washed with washing buffer for three times. Between each washing step, the product was separated by magnet and the supernate was discarded. Only the solid product was left in the centrifuge tube. Next, 20 μL phos-tag-biotin reaction buffer solution containing 10 μM phos-tag-biotin was added into the centrifuge tube and keep at 37 °C for 90 min under shaking. After that, the prepared composite (it was denoted as Fe_3O_4-5 hmC-Phos) was washed with washing buffer with the process as described above. Subsequently, 20 μL of 3 mg/mL avidin was added in the above tube and incubated at 37 °C for 1 h under shaking. After washing with washing buffer and discarded the supernate, 10 μL of 0.5 mg/mL EDC, 10 μL of 0.3 mg/mL NHS and 40 μL 4 mg/mL Ru was added into the tube and reacted at 37 °C for 2 h under shaking. The product was also washed with washing buffer and the complex was denoted as Fe_3O_4-5 hmC-Phos-Ru. Finally, 15 μL sterilized water was added into the tube to get homogeneous solution and the solution was transferred to the surface of electrode. After drying under infrared light, the electrode was rinsed with washing buffer for three times, and it was named as Fe_3O_4-5 hmC-Phos-Ru/GCE.

2.4. Real sample preparation

See Supplementary Material.

3. Results and discussion

3.1. Detection strategy

In this work, a novel and sensitive ECL biosensor was developed for 5 hmC detection based on the enzyme-catalytic covalent bonding reaction of $–CH_2OH$ and –SH, the specific reaction between phos-tag-biotin and phosphate group, the specific interaction between biotin and avidin, and the remarkable ECL performance of Ru. The detection progress and detection strategy were depicted in Scheme 1. Firstly, Fe_3O_4 nanosphere was prepared by the hydrothermal method. Then, a thin and uniform PDA film was coated on the surface of Fe_3O_4. Here, PDA plays three roles. Firstly, the cladding of PDA on Fe_3O_4 surface can prevent the absorption of Fe_3O_4 to 5 hmC through the interaction between Fe_3O_4 and the phosphate group of 5 hmC, phosphate group, which can effectively improve the detection selectivity. Secondly, PDA possesses active vicinal diol structure, which can facilitate the further surface modification of the composite. Thirdly, as a kind of biomolecule, dopamine widely exists in various organism, which lead to the good biocompatibility of PDA, improving the followed enzymatic reaction environment. Afterwards, –SH was further introduced on the Fe_3O_4 surface by the reaction between vicinal diol of PDA and boracic acid of MPBA. Subsequently, 5 hmC was captured on the surface of Fe_3O_4 by the enzyme-catalytic covalent bonding reaction of $–CH_2OH$ and –SH. After that, the phos-tag-biotin and avidin were immobilized successively on Fe_3O_4 surface by the specific reaction between phos-tag and phosphate group, and the specific interaction between biotin and avidin, respectively. Finally, the Ru was fixed on the surface of Fe_3O_4 based on the reaction between –COOH of avidin and $–NH_2$ of Ru to produce a strong ECL response. Moreover, all the reactions were carried out in the solution to ensure the activity of the biomolecules and the full progress of the reaction. Because the ECL response was quantitatively related to 5 hmC concentration, the biosensor can achieve the sensitive detection of 5 hmC.

3.2. Characterization of materials

The crystalline structures of Fe_3O_4 was characterized by XRD. As shown in Fig. 1A, all the peaks of the prepared sample are indexed to the Fe_3O_4 (PDF#89–4319), indicating the successful preparation of Fe_3O_4. In order to prove the successful modification of –SH, the Fe_3O_4 and Fe_3O_4-SH were characterized by EDS. As seen in Fig. 1B, the Fe_3O_4 only appears Fe and O peak. However, there are B, C, N, O, S, Fe peaks in the EDS pattern of Fe_3O_4-SH, indicating the successful modification of –SH (Fig. 1C). The morphology of the Fe_3O_4 and Fe_3O_4-SH was examined by SEM and TEM. The Fe_3O_4 and Fe_3O_4-SH were all spherical structure (Fig. 1D and E). As illustrated in Fig. 1F and G, an intact, uniform and thin film was coated on the surface of Fe_3O_4 after modification of –SH, which further demonstrated the successful modification of –SH.

3.3. Characterization of electrode modification

EIS is a typical tool for monitoring the electrode modification process. So, the preparation of Fe_3O_4-5 hmC-Phos-Ru/GCE was characterized by EIS in 10 mM PBS (pH 7.5) containing 5 mM $Fe(CN)_6^{3-/4-}$ and 0.1 M KCl. The EIS measurements were conducted covering the frequency range of 0.1–100 kHz in 5 mV amplitude of sinusoidal potential perturbation. As shown in Fig. 2A, the bare GCE shows a small semicircle in the high frequency region (R_{et}, 180 Ω, curve a). After the Ru-5 hmC-Fe_3O_4-SH was immobilized on the electrode, the R_{et} increased to 760 Ω (curve b). It can be attributed to the steric hindrance effect of Fe_3O_4-based composite, which can block the diffusion of $Fe(CN)_6^{3-/4-}$. The result proved that the Ru-5 hmC-Fe_3O_4-SH was fixed on the electrode successfully.

3.4. Detection feasibility assay

In order to testify the feasibility of the biosensor for 5 hmC detection, the ECL intensity of the different electrodes was detected. As seen in Fig. 2B, the bare GCE had no ECL response (curve a). When the Fe_3O_4-5 hmC-Phos-Ru composite was immobilized on the electrode, the ECL intensity increased strongly (curve b, c). Moreover, the ECL intensity increased with the increase of the 5 hmC concentration from 1 to 100 nM. To prove the important role of 5 hmC for capturing Ru, one control experiment was performed. Firstly, Fe_3O_4-SH was incubated directly with M. HhaI, phos-tag-biotin, avidin and Ru. Then, the Fe_3O_4-SH was washed and dropped on the electrode surface. After drying, the ECL response of the electrode was detected. As shown in Fig. 2B, the ECL intensity of the electrode is much lower than that measured for Fe_3O_4-5 hmC-Phos-Ru/GCE. This result demonstrated that Ru cannot immobilized on the electrode in the absence of 5 hmC. These results demonstrated that the biosensor can achieve the detection for 5 hmC.

3.5. Optimization of detection conditions

To achieve the better performance of the biosensor, some experimental conditions were optimized, including M. HhaI reaction time, phos-tag-biotin reaction time, avidin reaction time and Ru immobilization time. In order to optimize these experimental conditions, the Fe_3O_4-5 hmC-Phos-Ru/GCE was prepared and detected by the ECL analytical system, under different experimental conditions. The results were shown in Fig. S1.

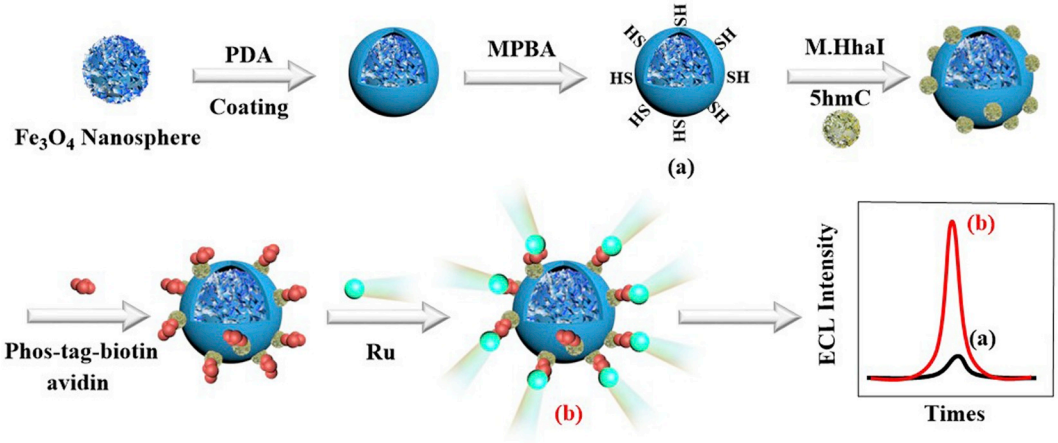

Scheme 1. Schematic illustration of the ECL biosensor construction process and 5 hmC detection.

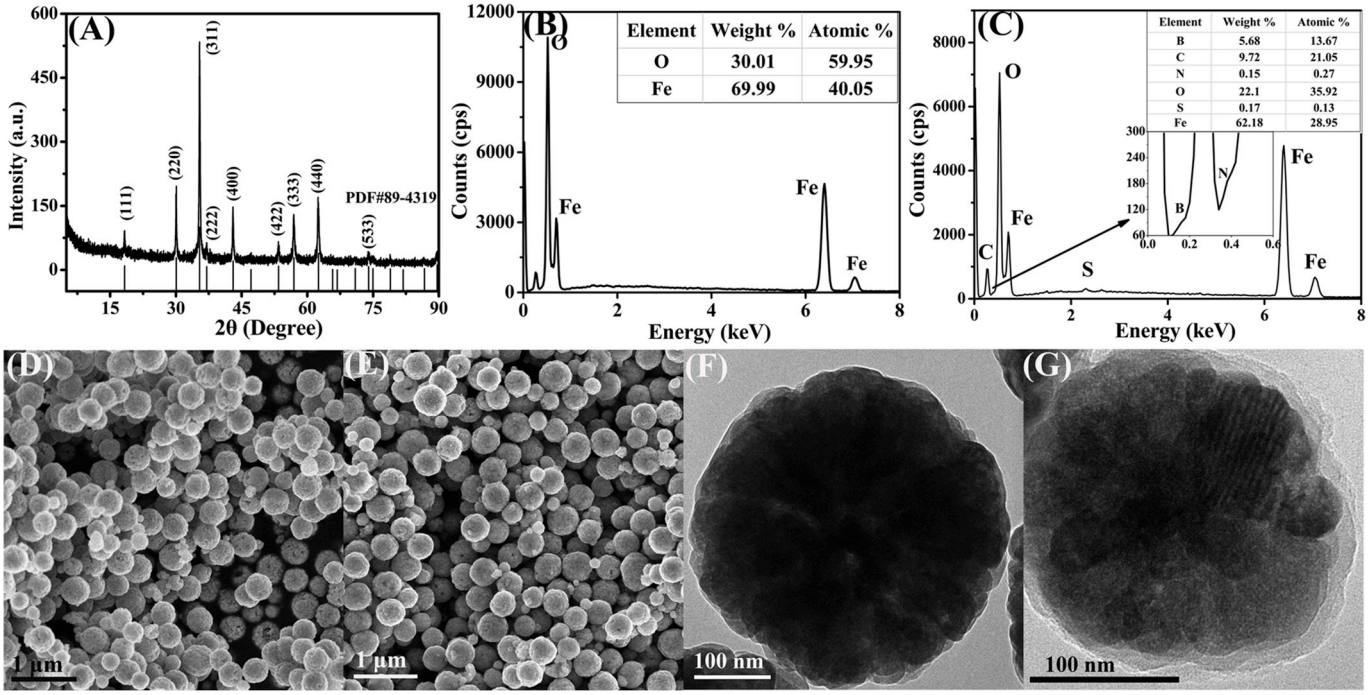

Fig. 1. (A) XRD pattern of Fe_3O_4, (B) and (C) EDS patterns of Fe_3O_4 and Fe_3O_4-SH, (D) and (E) SEM images of Fe_3O_4 and Fe_3O_4-SH, (F) and (G) TEM images of Fe_3O_4 and Fe_3O_4-SH.

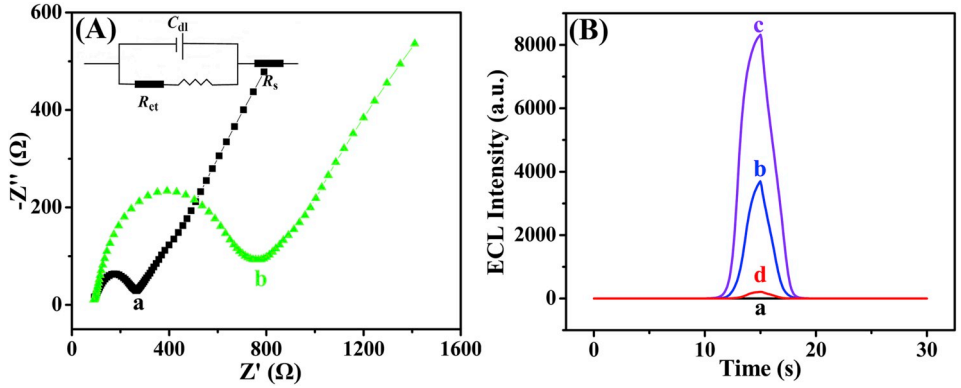

Fig. 2. (A) EIS of GCE (a), Fe_3O_4-5 hmC-Phos-Ru/GCE (b) in 5 mM K_3 [$Fe(CN)_6$]/K_4 [$Fe(CN)_6$] (1:1) containing 0.1 M KCl. (B) ECL-time curves of GCE (a), Fe_3O_4-5 hmC-Phos-Ru/GCE (1 nM 5 hmC) (b), Fe_3O_4-5 hmC-Phos-Ru/GCE (100 nM 5 hmC) (c), Fe_3O_4-SH incubated with phos-tag-biotin, avidin and Ru/GCE (d) in 10 mM PBS containing 100 mM $K_2S_2O_8$ (pH = 7.4).

As presented in Fig. S1A, the ECL intensity was increased with the increase of the M. HhaI reaction time from 20 to 140 min. Then, the ECL intensity increased slowly with further prolonging the catalysis time to 180 min, which can be attributed to the saturated reaction of 5 hmC with –SH on Fe_3O_4 surface. So, 140 min was selected as the M. HhaI reaction time.

Phos-tag-biotin and avidin were the linkers to capture the Ru-containing molecule, so the reaction time of phos-tag-biotin and avidin can influence the ECL intensity. As seen in Fig. S1B and Fig. S1C, the ECL intensity was increased with the increase of the reaction time. When the time to a threshold, the ECL intensity increased slowly, which can be explained that the reaction reached saturation. Therefore, 90 and 60 min were employed as the phos-tag-biotin reaction time and avidin reaction time, respectively.

Ru is the luminescent group, and the ECL intensity is dependent on the immobilization of Ru. Thus, the Ru immobilization time plays an important role in the performance of the biosensor. As illustrated in Fig. S1D, the ECL intensity increased with the increase of the Ru immobilization time from 20 to 120 min. Then, a plateau was achieved with further prolonging the immobilization time to 160 min. Thus, 160 was used as Ru immobilization time.

3.6. Detection performance

To testify the analytical performance of the biosensor, the ECL intensity of different concentrations of 5 hmC was measured and compared. As shown in Fig. 3A, under optimal conditions (see supporting information), the ECL intensity increased with changing 5 hmC concentration from 0.01 to 500 nM. A linear curve was obtained between the ECL intensity and the logarithm value of 5 hmC concentration (Fig. 3B), and the regression equation was I_{ECL} = 2094.70 log*c* (nM) + 4205.41 (R = 0.9974). The detection limit was calculated to be 2.86 pM (S/N = 3). Moreover, the detection performance of the biosensor was compared with previous reports and the results were listed in Table 1. Though the detection limit of this work is a little higher than that obtained at electrochemical and ECL method, these methods can only

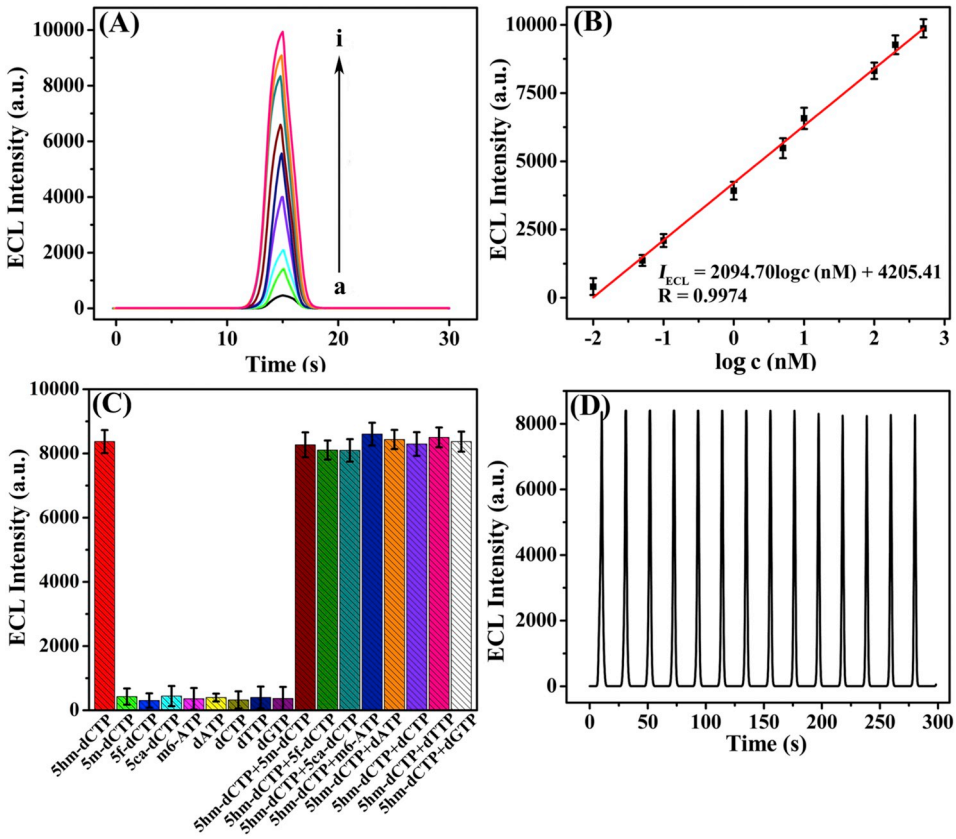

Fig. 3. (A) ECL intensity of the biosensor with different concentrations of 5 hmC. a-i, 0.01, 0.05, 0.1, 1, 5, 10, 100, 200, 500 nM. (B) The linear relationship between ECL intensity versus 5 hmC concentration. (C) The ECL intensities of the biosensor after it was incubated with different deoxyribonucleotides. (D) Continuous cyclic scans of the proposed ECL biosensor.

Table 1
Performance comparison of the ECL biosensor with other methods for 5 hmC detection.

Methods	Target	Linear range	LOD	Refs
Capillary electrophoresis	5 hmC-DNA	0.09–90 nM	0.09 nM	Krais et al. (2011)
Electrochemistry	5 hm-dCTP	0.1–30 nM	32 pM	Yang et al. (2015)
Electrochemistry	5 hmC-DNA	0.01–1000 pM	9.06 fM	Cui et al. (2019)
Fluorescence	5 hmC-DNA	0–100 nM	0.167 nM	Chen et al. (2017)
Fluorescence	5 hmC-DNA	0–150 nM	–	Hong et al. (2013)
Photoelectrochemistry	5 hmC-DNA	0.01–100 nM	3.40 pM	Sui et al. (2019)
Photoelectrochemistry	5 hm-dCTP	0.01–100 nM	4.12 pM	Zhou et al. (2019)
ECL	5 hm-dCTP	0.1–30 nM	0.047 nM	Jiang et al. (2018)
ECL	5 hmC-DNA	0.5–100 pM	0.14 pM	Ma et al. (2016)
ECL	5 hmC-DNA	0.01–1000 pM	3.84 fM	Wei et al. (2017)
ECL	5 hmC-DNA	0.05–10 pM	12 fM	Sun et al. (2019)
ECL	5 hm-dCTP	0.01–500 nM	2.86 pM	This work

detect 5 hmC contained short DNA sequence, which limits the application of these method for detecting 5 hmC in genomic DNA. In traditional biosensors, they are focusing on the detection of 5 hmC in a DNA sequence. However, the single-stranded bases and lengths in animals and plants are unknown, it is difficult to detect 5 hmC in actual animals and plants. Moreover, biomolecules are modified on the electrodes by layer assembly in traditional ECL biosensors. The capture efficiency is low due to the steric effect of the electrode surface and the influence of biomolecule activity. In this work, we used the functional Fe_3O_4 to transfer the reaction in the solution to achieve the sensitive detection of 5 hmC.

Selectivity is one of the critical factors for the performance of a biosensor, so 5 m-dCTP, 5f-dCTP, 5ca-dCTP, m6-ATP, dATP, dCTP, dTTP and dGTP were used as the interferents to examine the selectivity. In the process for preparing Fe_3O_4-5 hmC-Phos-Ru composite, 100 nM 5 hm-dCTP was replaced by the same concentration of the interferents. Then, the obtained Fe_3O_4-based composite was used to construct the biosensor and the ECL intensity of the biosensor was detected and compared. As illustrated in Fig. 3C, the ECL intensity of the Fe_3O_4-5 hmC-Phos-Ru/GCE was great higher than that for other interferents. The result proved the remarkable selectivity of the biosensor. Moreover, the photocurrent of 5 hm-dCTP is similar to the mixture of 5 hm-dCTP and other interferents. These results further demonstrate that the developed method has high detection specificity.

As an important parameter for biosensor performance, the stability was investigated and presented in Fig. 3D. The ECL intensity of the biosensor had no significant change under 14 repetitions continuous cyclic scans. The relative standard deviation (RSD) of the ECL response was only 1.02%, indicating the superior stability of the biosensor. The reproducibility of biosensor was also testified by comparing the ECL intensity of the seven Fe_3O_4-5 hmC-Phos-Ru/GCE prepared with the same condition (Fig. S5). There was no significant difference in the ECL intensity, the RSD was 2.56%, indicating an excellent stability.

3.7. Detection of 5 hmC in samples

In order to investigate the practical applicability of the biosensor, the 5 hmC content in the genomic DNA of rice seedling treated with different antibiotics (amoxicillin, tobramycin, chloramphenicol) and Cd^{2+} complex pollutants were measured by this biosensor. As seen in Fig. 4A, the 5 hmC content in the genomic DNA of rice seedling roots decreased with the treating of antibiotics and Cd^{2+} complex pollutants. Moreover, the 5 hmC content was lowest in the genomic DNA of rice seedling roots treated with tobramycin and Cd^{2+} complex pollutants. However, after the same treating, the 5 hmC content increased in the genomic DNA of rice seedling stems (Fig. 4B). In addition, the 5 hmC content was highest in the genomic DNA of rice seedling stems treated with tobramycin and Cd^{2+} complex pollutants. In the leaves, the 5 hmC level of rice seedling treated by amoxicillin and Cd^{2+} complex pollutants, chloramphenicol and Cd^{2+} complex pollutants increased, and the 5 hmC level of rice seedling treated by tobramycin and Cd^{2+} complex pollutants decreased slightly (Fig. 4C). The result demonstrated that the antibiotic and Cd^{2+} complex pollutants can affect the form of 5 hmC. This study may provide a new marker for the evaluation of the ecotoxicological effects of antibiotics and Cd^{2+} complex pollutants towards rice.

Avian leukemia is an avian disease caused by viruses of avian type C retroviruses, which can cause chicken immunosuppression, reduced ability to respond to vaccines, secondary infections and even death to cause huge economic losses. Moreover, there is no method to eradicate avian leukemia until now. The best way to minimize the impact of avian leukemia was the separation of infected chickens from the healthy chickens. So, the fast detection of the infected chickens was important. 5 hmC was considered as the sixth base of DNA, which plays important roles in life activity of animals. In addition, the level of 5 hmC decreased strongly in some cancers. Thus, we could use 5 hmC as the mark to achieve the detection of infected chickens. In order to prove the idea, the 5 hmC content in the genomic DNA of chicken fibroblasts cell after infected with ALV-J was investigated. As shown in Fig. 4D, the relative expression of 5 hmC decreased by infecting ALV-J. Moreover, the relative expression of 5 hmC decreased with the increase of the incubation time from 24 h to 72 h. The result further proved that the 5 hmC may be a new biomarker for the Avian leukemia.

In order to testify the accuracy of the biosensor, the detection results were also compared with that by MethylFlash Global DNA Hydroxymethylation (5 hmC) ELISA Easy Kit (Epigentek, USA). As illustrated in Fig. 4, there is almost no difference in the results of the two methods, indicating the superior practicability of the biosensor. We also performed a statistical analysis of the data of the sample test and the results were in line with expectations (See Supplementary Material).

4. Conclusion

In summary, a sensitive and low-cost ECL biosensor was fabricated for 5 hmC detection. In this work, a functional magnetic bead was prepared as the captured unit and separation medium of 5 hmC to achieve the homogeneous reaction. The method showed excellent detection performance, with a wide linear range from 0.01 to 500 nM and a low LOD of 2.86 pM. Moreover, the 5 hmC content in chicken embryo fibroblast cell was successfully detected by this biosensor, demonstrating that 5 hmC may be used as a biomarker for monitoring the effect of pollutants on crops and detecting Avian leukemia. However,

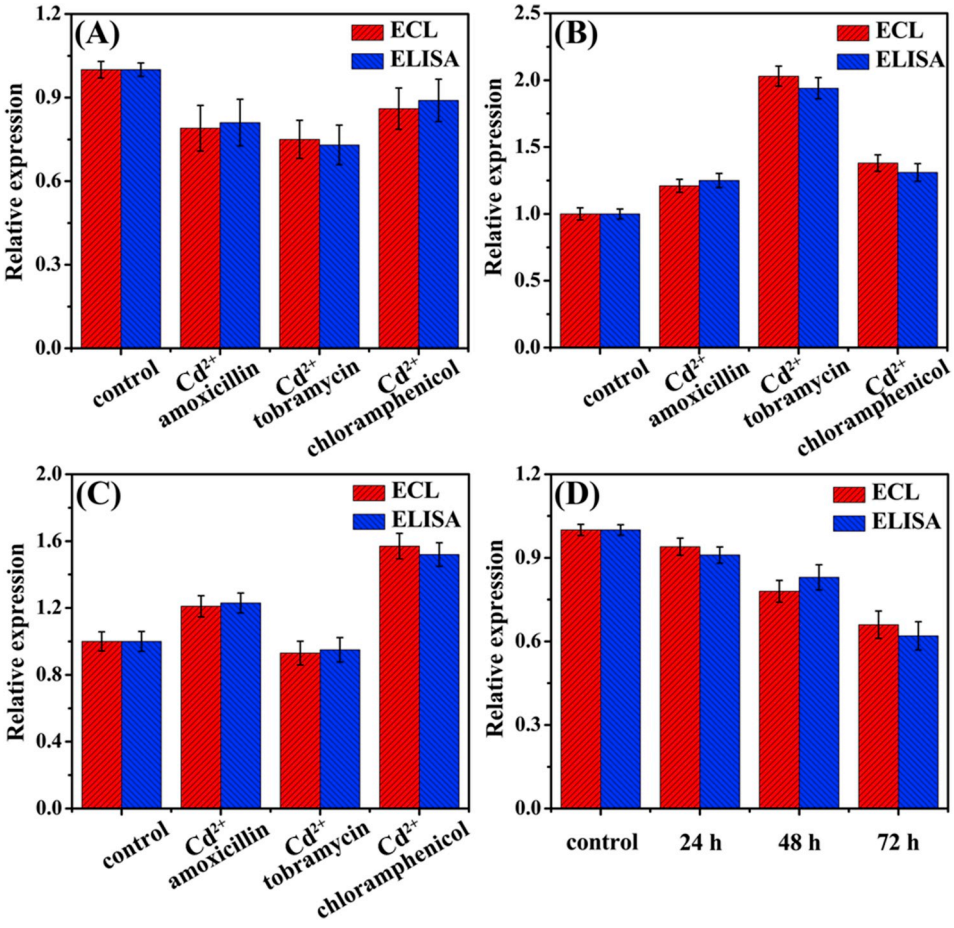

Fig. 4. Effect of different antibiotics and Cd^{2+} complex pollutants on 5 hmC expression in the genomic DNA of rice seedling roots (A), stems (B) and leaves (C). Effect of ALV-J on 5 hmC expression in the genomic DNA of chicken embryo fibroblast cell for 24, 48, 72 h (D).

the sample preparation progress and biosensors preparation progress need multiple steps, so in our future work, simplifying sample preparation steps and sensor preparation steps and improving sensor sensitivity are important part.

Author contribution statement

All the authors have been contributed for this work.

All the authors have been have made a significant contribution to the conception, design, execution, or interpretation of the reported study.

Declaration of competing interest

The authors declare that they have no known competing financial interests or personal relationships that could have appeared to influence the work reported in this paper.

CRediT authorship contribution statement

Chengji Sui: Conceptualization, Data curation, Investigation, Writing - original draft. **Huanshun Yin:** Conceptualization, Funding acquisition, Investigation, Project administration, Writing - review & editing. **Lingsong Wang:** Data curation, Investigation, Validation, Writing - original draft. **Yunlei Zhou:** Data curation, Funding acquisition, Investigation, Writing - original draft. **Shiyun Ai:** Conceptualization, Funding acquisition, Investigation, Supervision, Writing - review & editing.

Acknowledgements

This work was supported by the Natural Science Foundation of Shandong Province of China (No. ZR2018MB028), the National key research and development project of China (2018YFC1800605), the National Natural Science Foundation of China (Nos. 21775090, 41807484).

Appendix A. Supplementary data

Supplementary data to this article can be found online at https://doi.org/10.1016/j.bios.2019.111908.

References

Cai, J., Chen, T., Xu, Y., Wei, S., Huang, W., Liu, R., Liu, J., 2019. Biosens. Bioelectron. 124–125, 15–24.
Chen, H.-y., Wei, J.-R., Pan, J.-X., Zhang, W., Dang, F.-q., Zhang, Z.-Q., Zhang, J., 2017. Biosens. Bioelectron. 91, 328–333.
Chen, K., Zhang, J., Guo, Z., Ma, Q., Xu, Z., Zhou, Y., Xu, Z., Li, Z., Liu, Y., Ye, X., Li, X., Yuan, B., Ke, Y., He, C., Zhou, L., Liu, J., Ci, W., 2015. Cell Res. 26, 103.
Cui, L., Hu, J., Wang, M., Li, C.-c., Zhang, C.-y., 2019. Anal. Chem. 91, 1232–1236.
Deng, H., Li, X., Peng, Q., Wang, X., Chen, J., Li, Y., 2005. Angew. Chem. 117, 2842–2845.
Feng, Q., Wang, M., Zhao, X., Wang, P., 2018. Langmuir 34, 10153–10162.
Flusberg, B.A., Webster, D.R., Lee, J.H., Travers, K.J., Olivares, E.C., Clark, T.A., Korlach, J., Turner, S.W., 2010. Nat. Methods 7, 461.
Gao, F., Zhou, F., Chen, S., Yao, Y., Wu, J., Yin, D., Geng, D., Wang, P., 2017. Analyst 142, 4308–4316.
Ge, L., Sun, X., Hong, Q., Li, F., 2017. ACS Appl. Mater. Interfaces 9, 32089–32096.
Hong, T., Wang, T., Guo, P., Xing, X., Ding, F., Chen, Y., Wu, J., Ma, J., Wu, F., Zhou, X., 2013. Anal. Chem. 85, 10797–10802.
Hu, G.-B., Xiong, C.-Y., Liang, W.-B., Yang, Y., Yao, L.-Y., Huang, W., Luo, W., Yuan, R., Xiao, D.-R., 2019. Biosens. Bioelectron. 135, 95–101.
Jiang, W., Wu, L., Duan, J., Yin, H., Ai, S., 2018. Biosens. Bioelectron. 99, 660–666.
Krais, A.M., Park, Y.J., Plass, C., Schmeiser, H.H., 2011. Epigenetics 6, 560–565.
Li, N., Hao, X., Kang, B.H., Xu, Z., Shi, Y., Li, N.B., Luo, H.Q., 2016. Biosens. Bioelectron. 77, 525–529.
Li, X., Zhu, L., Zhou, Y., Yin, H., Ai, S., 2017. Anal. Chem. 89, 2369–2376.
Lin, X., Luo, F., Zheng, L., Gao, G., Chi, Y., 2015. Anal. Chem. 87, 4864–4870.
Liu, Z., Qi, W., Xu, G., 2015. Chem. Soc. Rev. 44, 3117–3142.
Liutkevičiūtė, Z., Kriukienė, E., Grigaitytė, I., Masevičius, V., Klimašauskas, S., 2011. Angew. Chem. Int. Ed. 50, 2090–2093.
Long, D., Shang, Y., Qiu, Y., Zhou, B., Yang, P., 2018. Biosens. Bioelectron. 102, 553–559.
Lu, J., Yan, M., Ge, L., Ge, S., Wang, S., Yan, J., Yu, J., 2013. Biosens. Bioelectron. 47, 271–277.
Lu, L., Su, H., Li, F., 2017. Anal. Chem. 89, 8328–8334.
Ma, S., Sun, H., Li, Y., Qi, H., Zheng, J., 2016. Anal. Chem. 88, 9934–9940.
Miao, Y.-B., Ren, H.-X., Gan, N., Zhou, Y., Cao, Y., Li, T., Chen, Y., 2016. Biosens. Bioelectron. 86, 477–483.
Song, C.-X., Szulwach, K.E., Fu, Y., Dai, Q., Yi, C., Li, X., Li, Y., Chen, C.-H., Zhang, W., Jian, X., Wang, J., Zhang, L., Looney, T.J., Zhang, B., Godley, L.A., Hicks, L.M., Lahn, B.T., Jin, P., He, C., 2010. Nat. Biotechnol. 29, 68.
Sui, C., Wang, T., Zhou, Y., Yin, H., Meng, X., Zhang, S., Waterhouse, G.I.N., Xu, Q., Zhuge, Y., Ai, S., 2019. Biosens. Bioelectron. 127, 38–44.
Sun, H., Wang, H., Bai, W., Bao, L., Lin, J., Li, Y., 2019. Talanta 191, 350–356.
Sun, S., Jiang, K., Qian, S., Wang, Y., Lin, H., 2017. Anal. Chem. 89, 5542–5548.
Sun, X., Du, Y., Zhang, L., Dong, S., Wang, E., 2007. Anal. Chem. 79, 2588–2592.
Tahiliani, M., Koh, K.P., Shen, Y., Pastor, W.A., Bandukwala, H., Brudno, Y., Agarwal, S., Iyer, L.M., Liu, D.R., Aravind, L., Rao, A., 2009. Science 324, 930–935.
Wang, Y.-Z., Hao, N., Feng, Q.-M., Shi, H.-W., Xu, J.-J., Chen, H.-Y., 2016. Biosens. Bioelectron. 77, 76–82.
Wei, Y., Sun, H., Li, J., Zhang, Y., Li, Y., Lin, J., Wang, T., Zhou, M., 2017. J. Electroanal. Chem. 795, 123–129.
Yan, L.-g., Yang, K., Shan, R.-r., Yan, T., Wei, J., Yu, S.-j., Yu, H.-q., Du, B., 2015. J. Colloid Interface Sci. 448, 508–516.
Yang, Z., Jiang, W., Liu, F., Zhou, Y., Yin, H., Ai, S., 2015. Chem. Commun. 51, 14671–14673.
Yin, R., Mo, J., Lu, M., Wang, H., 2015. Anal. Chem. 87, 1846–1852.
Zhou, Y., Yin, H., Sui, C., Wang, Y., Ai, S., 2019. Chem. Eng. J. 357, 94–102.